Fast left ventricle tracking in CMR images using localized anatomical affine optical flow

Sandro Queirós [a,b,c,1], João L. Vilaça[a,d], Pedro Morais[a], Jaime C. Fonseca[c],
Jan D'hooge[b], Daniel Barbosa[a,d,1]

[a]ICVS/3B's - PT Government Associate Laboratory, Braga/Guimarães, Portugal
[b]Lab on Cardiovascular Imaging and Dynamics, KU Leuven, Belgium
[c]Algoritmi Center, School of Engineering, University of Minho, Guimarães, Portugal
[d]DIGARC – Polytechnic Institute of Cávado and Ave, Barcelos, Portugal

ABSTRACT

In daily cardiology practice, assessment of left ventricular (LV) global function using non-invasive imaging remains central for the diagnosis and follow-up of patients with cardiovascular diseases. Despite the different methodologies currently accessible for LV segmentation in cardiac magnetic resonance (CMR) images, a fast and complete LV delineation is still limitedly available for routine use.

In this study, a localized anatomically constrained affine optical flow method is proposed for fast and automatic LV tracking throughout the full cardiac cycle in short-axis CMR images. Starting from an automatically delineated LV in the end-diastolic frame, the endocardial and epicardial boundaries are propagated by estimating the motion between adjacent cardiac phases using optical flow. In order to reduce the computational burden, the motion is only estimated in an anatomical region of interest around the tracked boundaries and subsequently integrated into a local affine motion model. Such localized estimation enables to capture complex motion patterns, while still being spatially consistent.

The method was validated on 45 CMR datasets taken from the 2009 MICCAI LV segmentation challenge. The proposed approach proved to be robust and efficient, with an average distance error of 2.1 mm and a correlation with reference ejection fraction of 0.98 (1.9 ± 4.5%). Moreover, it showed to be fast, taking 5 seconds for the tracking of a full 4D dataset (30 ms per image). Overall, a novel fast, robust and accurate LV tracking methodology was proposed, enabling accurate assessment of relevant global function cardiac indices, such as volumes and ejection fraction.

Keywords: Cardiac cine MRI, left ventricle tracking, localized affine optical flow, global cardiac function

1. INTRODUCTION

Cardiovascular diseases (CVDs) are the leading cause of death in the world[1]. Among the different techniques used in daily cardiology practice for the diagnostic process of patients with CVDs, left ventricular (LV) global function assessment using non-invasive imaging modalities is of utmost importance.

Currently, cardiac magnetic resonance (CMR) imaging is considered the gold standard technique for such assessment due to its excellent accuracy and reproducibility[2, 3]. The quantification of clinically relevant indices, such as end-diastolic volume (EDV), end-systolic volume (ESV), stroke volume (SV), left ventricular mass (LVM) or ejection fraction (EF), is usually performed by manual contouring of the endocardial and epicardial boundaries of the LV in cine CMR images[4-6]. Such task is tedious, time consuming and unpractical for routine use[7], normally requiring between 6 and 20 minutes to segment both endo and epicardial boundaries in all slices from base to apex in the end-diastolic (ED) and end-systolic (ES) cardiac phases only[7-9]. Moreover, manual contouring in clinical practice is prone to intra- and inter-observer variability, as recently shown by Miller et al.[8].

---

[1]Further author information:
 Sandro Queirós: sandroqueiros@ecsaude.uminho.pt
 Daniel Barbosa: danielbarbosa@ecsaude.uminho.pt

Currently, several methodologies for LV segmentation in CMR images have already been proposed[7], ranging from weak prior methods[10, 11] to strong shape prior-based ones[12, 13]. Despite such multitude of available frameworks, one that is fast, automatic and has optimal boundaries delineation is still lacking, usually requiring manual correction of imperfect contours[7, 9]. To overcome such limitations, the authors proposed, in a previous publication, a novel fast 3D+time segmentation framework for LV CMR segmentation[14]. This framework consisted on three conceptual blocks: (1) an automatic initialization and segmentation of a mid-ventricular slice in the ED phase; (2) an automatic stack initialization followed by 3D myocardial segmentation; and (3) a tracking procedure for contours propagation throughout the full cardiac cycle. While the framework presented highly competitive results against state-of-the-art methods and excellent correlations with reference cardiac indices, the third module was found to be the least performing one. Indeed, the proposed framework[14] uses a global anatomical affine optical flow method, which propagates the boundaries assuming a global affine motion model between adjacent frames[15]. Although such propagation is performed slice by slice with a robust result for a multitude of motion patterns, it has difficulties in following local motion or deformation inhomogeneity of the myocardial wall. Therefore, this block remains a limitation of the framework towards a more localized assessment of LV function.

In order to improve the current framework and provide an accurate delineation of the LV, this study presents a novel localized anatomical affine optical flow method for LV tracking in short-axis (SAX) CMR images. Experiments in 45 datasets demonstrated the accuracy and robustness of the proposed method.

2. METHODS

2.1 Overview

A complete LV delineation is mandatory for comprehensive global left ventricular function analysis. In this study, the goal was to propagate a set of contours delineated in a given cardiac phase throughout the full cardiac cycle. Such delineation can be previously obtained either from a manual, semi-automatic or fully automatic contouring technique.

Hereto, we propose to start from a fully delineated LV surface at the ED frame obtained using the automatic method proposed by Queirós et al.[14] (briefly explained in Section 2.2), followed by its propagation by locally estimating the motion between adjacent cardiac phases. In the end, the relevant cardiac indices can be extracted from the automatically tracked LV surfaces (see Figure 1).

2.2 Automatic segmentation at the ED phase

In order to automatically delineate the myocardium at the ED phase, its initial detection is required. To this end, a LV localization algorithm[16], based on multi-level Otsu thresholding and elliptical object detection, is applied to a mid-ventricular SAX slice at the ED phase. After LV blood pool identification, an elliptical annular template matching algorithm[16] is employed for detection of the myocardium, taking advantage of its annular appearance in CMR SAX images. With the consecutive use of both methods, two elliptical contours, roughly delineating the endo and epicardial boundaries, are obtained. These contours are then refined using a coupled formulation of the recent B-Spline Explicit Active Surfaces (BEAS) framework[17], for which a specifically designed energy functional for CMR images, using localized region-based terms, was designed[14].

In a second stage, an extended 3D coupled BEAS segmentation, using a cylindrical topology, is applied to extract the full LV surface at the ED phase. Since an initialization is required, the image appearance information gathered from the initial mid-ventricular segmentation is used in a threshold-based BEAS to expand the mid-ventricular result to all slices from base to apex. After initialization, the surface is deformed towards positions of high local contrast, indicating
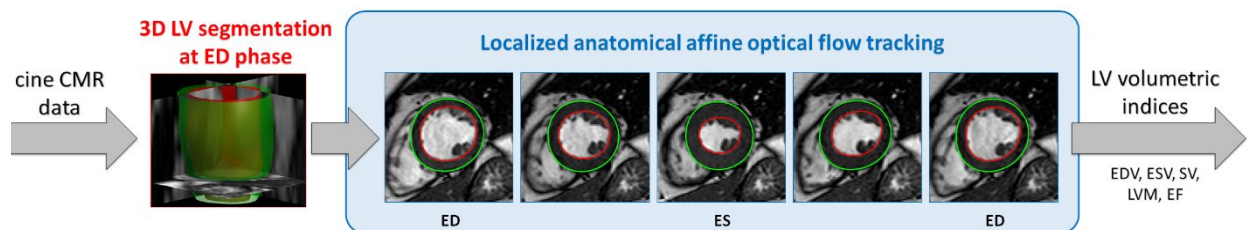

Figure 1. Overview of the proposed framework using localized anatomical affine optical flow tracking for complete LV delineation.

blood-tissue or tissue-outside interfaces, while also looking for edge content around the epicardial boundary. This hybrid region-based and edge-based energy functional proved to be robust and accurate for LV delineation[14]. Note that the BEAS framework implicitly guarantees the smoothness and spatial coherence of the extracted 3D surface, allowing to globally optimize its fit to the patient-specific dataset appearance without introducing local spatial irregularities on the segmented shape. Further technical details regarding the automatic LV segmentation framework can be found in Queirós *et al.*[14].

2.3 Localized anatomical affine optical flow tracking

Starting from the delineated LV surface in the ED frame, the goal is to propagate the contours throughout the full cardiac sequence by locally estimating the myocardial motion between adjacent frames. Similarly to Queirós *et al.*[14] and due to the anisotropy of the CMR data, such estimation is performed independently for each slice sequence and for each myocardial boundary (i.e. endo or epicardium).

Let $\Gamma_i(\theta)$ represent the myocardial wall boundary i (endo or epicardium) given as a function of the angle θ of a polar space centered at $\boldsymbol{c} = [c_1, c_2]$. The principle of the proposed approach is to locally estimate the motion for each contour point based on its location, $\boldsymbol{x} = [x_1, x_2]$, while also taking into account its angular position, θ, in the boundary Γ_i. Thus, the local motion field around $\Gamma_i(\theta)$ is encoded as:

$$u_\theta(x_1, x_2) = u_0 + u_1(x_1 - c_1) + u_2(x_2 - c_2) \tag{1}$$

$$v_\theta(x_1, x_2) = v_0 + v_1(x_1 - c_1) + v_2(x_2 - c_2) \tag{2}$$

Let $I(x_1, x_2, t)$ denote the pixel intensity at location $\boldsymbol{x}$ and time t for a given slice temporal sequence. Based on the least square solution of the optical flow equation, the 2D localized affine motion for a given contour point can be estimated by minimizing the following energy:

$$E_\theta = \int_{\mathbb{R}^2} W_\theta(x_1 - c_1, x_2 - c_2)(I_1 u_\theta + I_2 v_\theta + I_t)^2 d\boldsymbol{x} \tag{3}$$

where $\nabla I = [I_1, I_2]$ is the local image spatial gradient and I_t is the temporal derivative. In order to reduce noise sensitivity during spatial gradient assessment, $\nabla I(\boldsymbol{x})$ is computed using gaussian derivative kernels along each direction ($\sigma = 1$). I_t is simply computed with finite forward differences.

As originally proposed in Barbosa *et al.*[15], the estimation is confined to an anatomical region of interest (ROI) given by the initial surface and encoded by W_θ. However, in opposition to the global strategy[14, 15], we propose to integrate the estimated motion into a local displacement considering the neighbor regions and their angular distance to the point of interest (θ, measured assuming a polar space). Therefore, the ROI is given by:

$$W_\theta(x_1, x_2) = \sum_{x_k \in \Gamma_i} N(x_k) \times \left(\frac{1}{\sigma_\theta \sqrt{2\pi}} e^{-(\theta_k - \theta)^2 / (2\sigma_\theta^2)} \right) \tag{4}$$

where $N(\boldsymbol{x})$ is a neighborhood function defined as a 2D square centered in $\boldsymbol{x}$ and $x_k \in \Gamma_i$ stands for the sampled points in the LV boundary being tracked. N was defined as a 7×7 square centered in x_k. Note that to reduce the method's computational burden, the local motion displacement is computed in 16 equally-spaced points around the LV contour being tracked. σ_θ is given according to the desired support for the localized estimation ($3\pi/8$ rad in the current experiment). Thus, for each point in the boundary, a local affine motion model is estimated via a weighted anatomical ROI, in opposition to the global affine deformation originally estimated[14]. These differences are highlighted in Figure 2.

3. RESULTS

The approach was validated on 45 datasets taken from the 2009 MICCAI Cardiac MR LV segmentation challenge[18]. The datasets were obtained with a 1.5T GE Signa MRI using a cine steady state free precession (SSFP) pulse sequence, during 10- to 15-s breath holds. Six to twelve images were obtained from the atrioventricular ring to the apex (thickness = 8 mm, FOV = 320 mm $\times$ 320 mm, matrix = 256 $\times$ 256), with an isotropic pixel spacing ranging from 1.29 to 1.56 mm and a temporal resolution of 20 phases over the cardiac cycle. The database includes 36 patients (12 with heart failure and myocardial infarction, 12 with heart failure but no myocardial infarction and 12 with hypertrophic cardiomyopathy) and 9 normal cases. Moreover, a ground truth, drawn by an experienced observer, is available in all slices for the
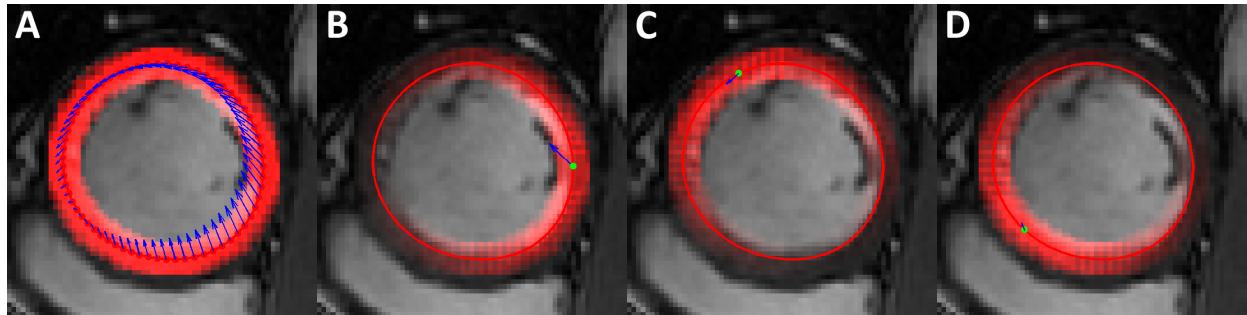
Figure 2. (A) Global anatomical affine optical flow[14] and (B-D) localized anatomical affine optical flow at 3 different angles. The solid line represents the contour being tracked, while the overlaid squares represent the anatomical region of interest. Blue arrows represent the motion displacement estimated (A) globally and (B-D) locally for each contour point (green point).

endocardium and epicardium at the ED phase and for the endocardium at the ES phase. All results consider manual contours drawn to include trabeculae and papillary muscles (TPMs) in the LV blood pool.

To evaluate the proposed approach, the tracking was applied to the ED LV surface obtained with the 3D coupled segmentation described in Section 2.2. A representative result of the tracking throughout a full cardiac cycle for different SAX slices is illustrated in Figure 3. The average computational time for the tracking of both endo and epicardial boundaries throughout all slices and frames was 4.98 ± 0.94 s (around 30 ms per image). The reported average computational time was obtained using a Matlab implementation running on a Intel (R) Core (TM) i5 CPU at 2.4 GHz (shared memory of 4GB).

The segmentation performance was assessed against reference contours using as metrics the Dice coefficient, the
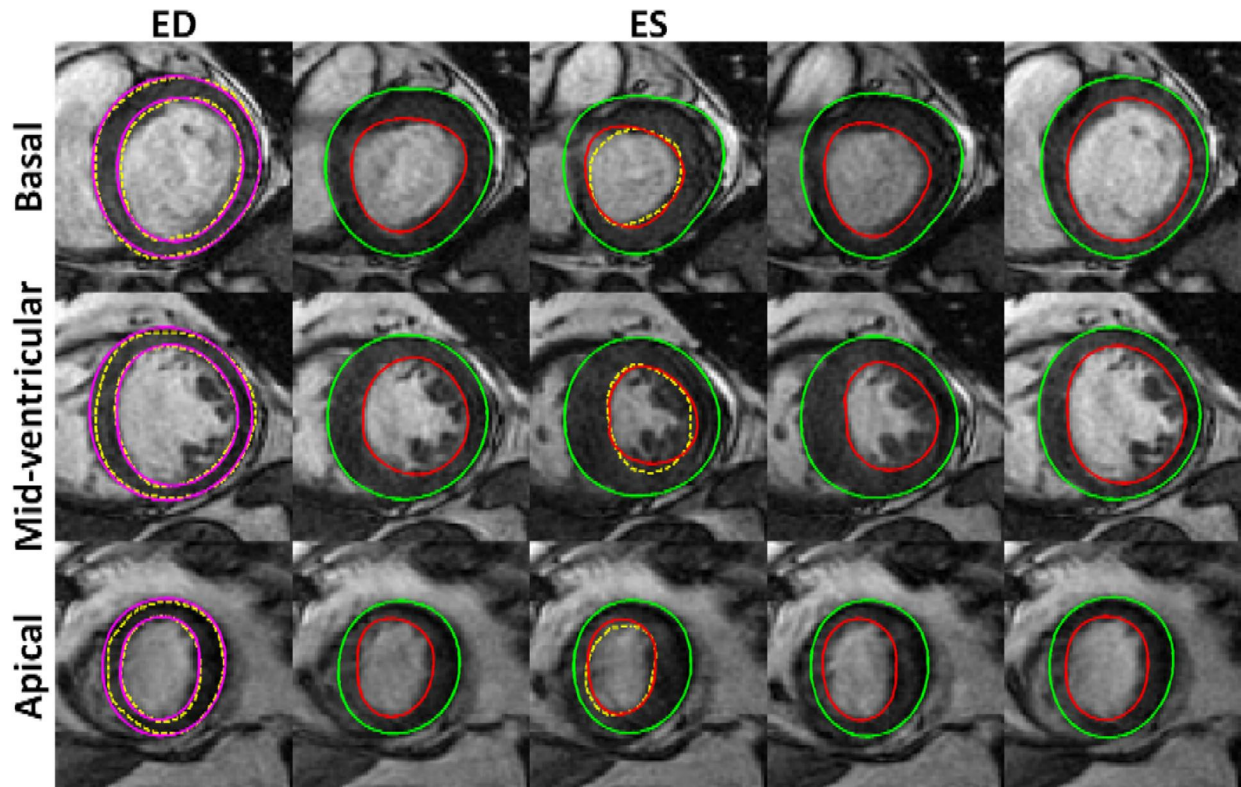

Figure 3. Localized anatomical affine optical flow tracking result for an example CMR dataset (magenta: automatic contour at ED phase; red – tracked endocardium; green – tracked epicardium; yellow – ground truth).

Table 1. 3D+time segmentation results for both endo and epicardial contours, between proposed approach and original method[14].

	Dice		APD (mm)		Hausdorff (mm)		Good contours (%)	
	Endo	Epi	Endo	Epi	Endo	Epi	Endo	Epi
[14]	0.87 ± 0.07	0.93 ± 0.03	2.14 ± 0.88	2.06 ± 0.84	5.05 ± 1.85	5.14 ± 1.79	92.7 ± 9.5	95.4 ± 9.6
Proposed	0.88 ± 0.06[a]		2.07 ± 0.84[a]		5.14 ± 1.88[a]		94.3 ± 8.5	

[a] $p < 0.05$, paired t-test against [14].

Table 2. Linear regression and Bland-Altman analysis for clinical cardiac indices with proposed approach and original method[14].

	EDV (mL)			ESV (mL)			SV (mL)			LVM (g)			EF (%)		
	R	Bias	σ	R	Bias	σ	R	Bias	σ	R	Bias	σ	R	Bias	σ
[14]	0.985	-2.46	15.03	0.988	-3.83	14.78	0.955	1.38	8.07	0.951	5.51[a]	14.13	0.976	3.00[a]	5.60
Proposed	0.989	-2.75[b]	13.66				0.962	0.30[b]	7.71				0.980	1.87[a,b]	4.54

R is the Pearson product-moment correlation coefficient.

[a] $p < 0.05$, paired t-test against zero.

[b] $p < 0.05$, paired t-test against [14].

average perpendicular distance (APD), the Hausdorff distance and the percentage of good contours (APD > 5 mm)[14].

Table 1 summarizes the performance for the complete 3D+time framework, as reported in Queirós *et al.*[14] and with the proposed localized anatomical affine optical flow as tracking module. Note that epicardial results are unchanged since no expert delineations are available at the ES phase (since only endocardial surface is needed for cardiac indices computation).

Finally, the computed cardiac indices were assessed against reference values to validate the approach in a clinical context. Table 2 presents the correlation coefficient obtained by regression analysis and both bias (average difference) and standard deviation obtained by Bland-Altman analysis for EDV, ESV, SV, LVM and EF. The corresponding plots are shown in Figure 4 and Figure 5. Overall, both EDV and ESV are underestimated, resulting in a slight overestimation of the left ventricular EF. LVM is overestimated, presenting the lowest correlation with manually computed indices. Note that in the Bland-Altman analysis the difference is calculated as the automatically computed value minus the reference one. Moreover, a two-tailed paired t-test was used to determine the statistical significant (p) of the differences found between automatically and manually computed indices. Our null hypothesis was that no difference exists, and p-
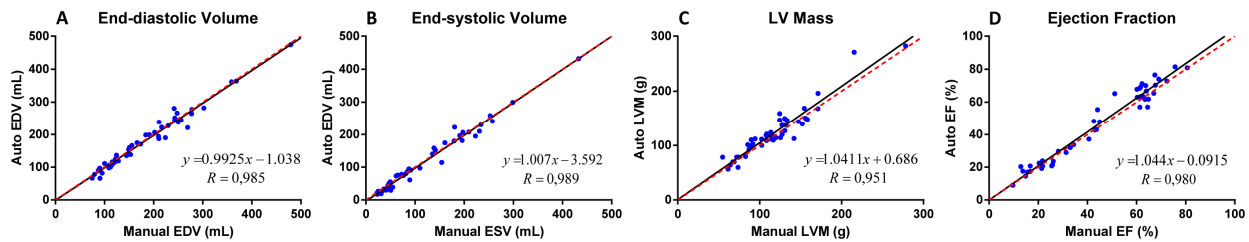

Figure 4. Linear regression for (A) end-diastolic volume (EDV); (B) end-systolic volume (ESV); (C) left ventricular mass (LVM); and (D) ejection fraction (EF) using the proposed localized anatomical affine optical flow tracking (red dashed line represents the obtained linear regression, while the black line illustrates the optimal regression).
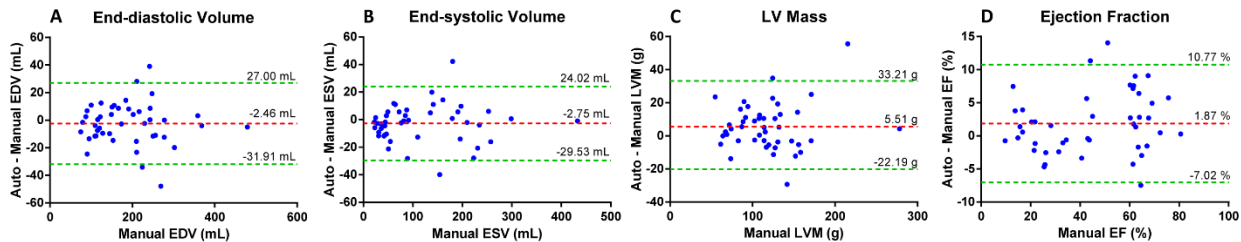

Figure 5. Bland-Altman plots for (A) end-diastolic volume (EDV); (B) end-systolic volume (ESV); (C) left ventricular mass (LVM); and (D) ejection fraction (EF) using the proposed localized anatomical affine optical flow tracking. Both bias (red dashed line) and limits of agreement (green dashed lines) are represented for clarity.

values ≤ 0.05 were considered statistically significant. The same statistical test was applied between the indices computed using the original and proposed tracking methods, showing statistically significant improvements for all relevant parameters when using the proposed localized motion estimation strategy.

4. DISCUSSION

The validation of the proposed method was performed on 45 CMR datasets, presenting robust and accurate results, as illustrated in Figure 3. The method presented an increased ability to capture local deformities when compared to the global affine version, without however losing spatial consistency or wrongly tracking the LV boundaries. Such ability is fundamental near TPMs, where a consistent position, relative to the neighborhood, should be kept throughout the SAX sequence. Since our automatic LV segmentation method at the ED phase excludes TPMs from the myocardium, the tracking should be able to keep them inside the blood pool as well. Although a localized tracking is performed, such result is still obtained with the proposed approach (see Figure 3 at the mid-ventricular level). At the same time, the localized ability of the current version allows to better capture local heterogeneity in myocardial motion and deformation, which occur in many pathological cases. For such reasons, the proposed methodology presented a superior accuracy when compared to its global counterpart, as can be observed in Table 1, with a statistically significant reduction in APD and a significant increase in the Dice metric. Notwithstanding, and as expected, the localized tracking method presents a superior average computational time than its global counterpart (average 4.98s vs 2.89s[14]). However, the difference is not significant for its potential application in daily clinical practice.

Although a sensitivity analysis is not presented in the current study, experiments showed that the localized tracking is able to correctly propagate the LV boundaries for a large range of values of the localized support parameter, σ_θ. Note that such parameter allows to choose from a single-point estimation (less robust and resulting in a more irregular result) to a full global support estimation (as in its global counterpart, being robust but less capable of local deformation capture). Thus, a trade-off between robustness and localized estimation exists when setting this parameter. In the current experiment, an intermediate value, illustrated in Figure 2B-D, is used to obtain a good balance between localized estimation and robustness. We intend to focus in the near future on how this parameter, σ_θ, can be automatically tuned to match the confidence degree on the local image information.

In the end, the proposed method allowed to achieve higher correlations with manually computed indices (Table 2), with reduced bias and limits of agreement (Figure 5). Once again, the proposed localized tracking showed statistically significant improvements compared to its global counterpart, with a final correlation of 0.99, 0.96 and 0.98 for ESV, SV and EF, respectively (Table 2 and Figure 4).

5. CONCLUSION

In this study, a novel localized anatomical affine optical flow method is proposed for fast LV tracking in cine SAX CMR images. The proposed method is intended to be used within an existing LV segmentation framework, allowing to propagate an initial LV surface throughout the full cardiac cycle and, thus, completely characterizing the LV morphology and function of a given patient. The approach allows to better capture local deformations of the myocardial wall, while being robust and spatially consistent. Overall, it showed significantly better results than its global counterpart, with an average distance error of 2.1 mm. In addition, the method is computationally efficient, taking around 5 seconds for the tracking of a full 4D dataset (30 ms per image). Finally, a high correlation with reference clinical cardiac indices was achieved when applying the complete framework, with 0.99 for ESV and 0.98 for EF with reduced biases and narrow limits of agreement.

6. ACKNOWLEDGEMENTS

REFERENCES

[1] World Health Organization, "Cardiovascular diseases," Fact sheet 317, (2012).

[2] C. A. Miller, K. Pearce, P. Jordan *et al.*, "Comparison of real-time three-dimensional echocardiography with cardiovascular magnetic resonance for left ventricular volumetric assessment in unselected patients," European Heart Journal–Cardiovascular Imaging*, 13(2), 187-195 (2012).

[3] F. Grothues, G. C. Smith, J. C. Moon *et al.*, "Comparison of interstudy reproducibility of cardiovascular magnetic resonance with two-dimensional echocardiography in normal subjects and in patients with heart failure or left ventricular hypertrophy," The American journal of cardiology*, 90(1), 29-34 (2002).

[4] K. Alfakih, S. Plein, H. Thiele *et al.*, "Normal human left and right ventricular dimensions for MRI as assessed by turbo gradient echo and steady-state free precession imaging sequences," Journal of Magnetic Resonance Imaging*, 17(3), 323-329 (2003).

[5] L. E. Hudsmith, S. E. Petersen, J. M. Francis *et al.*, "Normal human left and right ventricular and left atrial dimensions using steady state free precession magnetic resonance imaging," Journal of Cardiovascular Magnetic Resonance*, 7(5), 775-782 (2005).

[6] J. Caudron, J. Fares, V. Lefebvre *et al.*, "Cardiac MRI assessment of right ventricular function in acquired heart disease: Factors of variability," Academic Radiology*, 19(8), 991-1002 (2012).

[7] C. Petitjean, and J. N. Dacher, "A review of segmentation methods in short axis cardiac MR images," Medical image analysis*, 15(2), 169-184 (2011).

[8] C. A. Miller, P. Jordan, A. Borg *et al.*, "Quantification of left ventricular indices from SSFP cine imaging: Impact of real-world variability in analysis methodology and utility of geometric modeling," Journal of Magnetic Resonance Imaging*, 37(5), 1213-1222 (2012).

[9] G. L. Hautvast, C. J. Salton, M. L. Chuang *et al.*, "Accurate computer-aided quantification of left ventricular parameters: Experience in 1555 cardiac magnetic resonance studies from the Framingham Heart Study," Magnetic Resonance in Medicine*, 67(5), 1478-1486 (2012).

[10] L. Cordero-Grande, G. Vegas-Sánchez-Ferrero, P. Casaseca-de-la-Higuera *et al.*, "Unsupervised 4D myocardium segmentation with a Markov Random Field based deformable model," Medical image analysis*, 15(3), 283-301 (2011).

[11] I. Ben Ayed, H.-m. Chen, K. Punithakumar *et al.*, "Max-flow segmentation of the left ventricle by recovering subject-specific distributions via a bound of the Bhattacharyya measure," Medical image analysis*, 16(1), 87-100 (2012).

[12] A. Eslami, A. Karamalis, A. Katouzian *et al.*, "Segmentation by retrieval with guided random walks: Application to left ventricle segmentation in MRI," Medical image analysis*, 17(2), 236–253 (2012).

[13] H. Zhang, A. Wahle, R. K. Johnson *et al.*, "4-D cardiac MR image analysis: left and right ventricular morphology and function," Medical Imaging, IEEE Transactions on*, 29(2), 350-364 (2010).

[14] S. Queirós, D. Barbosa, B. Heyde *et al.*, "Fast automatic myocardial segmentation in 4D cine CMR datasets," Medical image analysis*, 18(7), 1115-1131 (2014).

[15] D. Barbosa, B. Heyde, T. Dietenbeck *et al.*, "Fast left ventricle tracking in 3D echocardiographic data using anatomical affine optical flow," Functional Imaging and Modeling of the Heart (FIMH2013)*. 7945, 191-199 (2013).

[16] S. Queirós, D. Barbosa, B. Heyde *et al.*, "Fast Fully Automated Segmentation of The Myocardium in 2D MR Images," Functional Imaging and Modeling of the Heart (FIMH2013)*. 7945, 71-79 (2013).

[17] D. Barbosa, T. Dietenbeck, J. Schaerer *et al.*, "B-Spline Explicit Active Surfaces: An Efficient Framework for Real-Time 3-D Region-Based Segmentation," Image Processing, IEEE Transactions on*, 21(1), 241-251 (2012).

[18] P. Radau, Y. Lu, K. Connelly *et al.*, "Evaluation framework for algorithms segmenting short axis cardiac MRI," MIDAS J.—Cardiac MR Left Ventricle Segmentation Challenge, (2009).